applied optics

Pixel-by-pixel absolute three-dimensional shape measurement with modified Fourier transform profilometry

HUITAEK YUN, BEIWEN LI, AND SONG ZHANG*

School of Mechanical Engineering, Purdue University, West Lafayette, Indiana 47907, USA
**Corresponding author: szhang15@purdue.edu*

Received 8 November 2016; revised 15 January 2017; accepted 15 January 2017; posted 17 January 2017 (Doc. ID 280456); published 9 February 2017

The single-pattern Fourier transform profilometry (FTP) and double-pattern modified FTP methods have great value in high-speed three-dimensional shape measurement, yet it is difficult to retrieve absolute phase pixel by pixel. This paper presents a method that can recover absolute phase pixel by pixel for the modified FTP method. The proposed method uses two images with different frequencies, and the recovered low-frequency phase is used to temporally unwrap the high-frequency phase pixel by pixel. This paper also presents the computational framework to reduce noise impact for robust phase unwrapping. Experiments demonstrate the success of the proposed absolute phase recovery method using only two fringe patterns.

OCIS codes: (120.0120) Instrumentation, measurement, and metrology; (100.5088) Phase unwrapping; (110.5086) Phase unwrapping; (100.5070) Phase retrieval.

https://doi.org/10.1364/AO.56.001472

1. INTRODUCTION

There are huge demands for three-dimensional (3D) shape measurements from the manufacturing industry to the biomedical area. Among 3D measurement methods, phase-based approaches have advantages over intensity-based ones due to their robustness to noise and the ability to achieve pixel level resolution. Fourier transform profilometry (FTP) [1], as one of the phase-based methods, can obtain a phase map from a single fringe pattern. The FTP method has been widely used for high-speed 3D shape measurement [2,3], such as instantaneous deformation measurements [4] and vibration of micro-mechanical device measurements [5]. However, it is challenging to achieve high measurement quality with a single pattern due to the impact of the DC component (e.g., ambient lighting, surface texture). Guo *et al.* [6] developed a modified FTP method to improve measurement quality by adding one more phase-shifted fringe pattern with the same period that it reduced the impact of the DC component.

In general, the FTP method retrieves only relative phase due to the use of a spatial phase-unwrapping algorithm. It is well known that the spatial phase unwrapping cannot be employed for simultaneous measurements of multiple spatially isolated objects or ones with abrupt surface geometric changes (e.g., cause more than π phase changes from one pixel to the next). To obtain absolute phase, different markers were used to carry unique phase value from which the spatially unwrapped phase can be converted to absolute phase. For example, Guo and Huang [7] encoded a cross-shaped marker on the projected fringe pattern, and located the marker from the captured fringe pattern; Budianto *et al.* [8] embedded stripe markers to the projected sinusoidal pattern, and retrieved the marker stripe through the wavelet transform. However, these marker-based approaches work only when the marker is clearly visible within the connected patches; the methods cannot work if a spatially isolated object does not have the visible marker on it, or the object has abrupt surface changes.

Temporal phase unwrapping can recover absolute phase for multiple isolated objects and ones with abrupt surface geometric changes. Conventional laser interferometry employs two-frequency phase-shifting methods for temporal phase unwrapping [9], and the digital fringe projection (DFP) technique allows adding a single period of fringe patterns that covers the whole sensing area for temporal phase unwrapping [10]. These two-frequency phase-shifting approaches can work well if the noise is not large [11]. When the noise is large, typically, multi-wavelength phase-shifting techniques [12,13] are more desirable for laser interferometry or a DFP system. Alternatively, binary- or gray-coding [14,15] can also be used for temporal phase unwrapping. In general, temporal phase-unwrapping methods require more than two additional fringe patterns to perform pixel-by-pixel absolute phase recovery. For high-speed applications, it is not desirable to use many fringe patterns.

In short, the 3D shape measurement technique based on a spatial phase-unwrapping method has the speed advantage since it requires only one or two fringe patterns; yet, it is difficult for such a method to recover absolute phase pixel by pixel. In contrast, the 3D shape measurement technique based on temporal phase unwrapping can measure absolute geometry pixel by pixel, yet it substantially reduces the measurement speed by requiring at least two more fringe patterns.

To address the limitations of existing spatial and temporal unwrapping methods, some researchers have recently started to use the geometric constraints of a DFP system to assist phase unwrapping. Hyun and Zhang [16] used the geometric constraints to enhance the performance of the two-frequency phase-shifting method. This method reduces the scaling ratio between high- and low-frequency phase so that the method can minimize the impact of phase noise. However, the method still uses six fringe images, three phase-shifted patterns for each frequency, which is not desirable for high-speed measurement applications. The method proposed by An *et al.* [17] unwrapped the phase obtained from a three-step phase-shifting technique solely using the geometric constraints. To reduce the number of fringe patterns required for 3D shape measurement, Li *et al.* [18] employed this technique to unwrap phase that is obtained from a single-shot FTP method. This method has enabled absolute phase retrieval from a single-shot 8 bit fringe image. However, in general, the geometric-constraint-based phase-unwrapping method has one fundamental limitation: the maximum depth range is roughly proportional to the fringe period used [17]. Therefore, the single-shot FTP method that Li *et al.* [18] developed has a very small depth range since the fringe period used is very small.

This paper presents a novel method that requires only two fringe patterns for pixel-by-pixel absolute phase recovery. The proposed method is similar to the modified FTP method proposed by Guo *et al.* [6] in that we also use two fringe patterns to reduce the impact of the DC component and apply the Fourier transform method to retrieve the phase. However, our method differs from the method proposed by Guo *et al.* [6] because (1) we use two different frequencies instead of the same frequency for these two fringe patterns; (2) we realize a temporal phase unwrapping for pixel-by-pixel absolute phase recovery, yet Guo *et al.*'s method recovers only the relative phase since the spatial phase-unwrapping method is adopted; and (3) our method could have a lower phase quality because a low-frequency component can affect the effective bandwidth of the high-frequency component. Conceptually, the proposed method works as follows: (1) we apply Fourier transform to the difference images of these two fringe patterns, (2) we use the bandpass filters to separate the low-frequency and high-frequency components, (3) we compute the wrapped phase for both frequency components, and (4) finally we unwrap the high-frequency phase pixel by pixel by referring to the low-frequency phase. Because the existence of two frequency components on the difference image, it is desirable to separate these two frequencies as far away as possible for accurate bandpass filtering. In other words, for a given high fringe frequency, we would like to make the low frequency as close to the DC component as possible. However, if the single low-frequency fringe spans the entire field of view, our research finds that the FTP method fails to accurately recover phase if a complex object is captured. Of course, this allows changes to the temporal phase unwrapping since the ratio between high and low frequency is too large. In other words, practically, the low frequency cannot be as low as a single fringe that covers the entire projection range. We overcome this dilemma by using more than one period of low-frequency fringe patterns, and by employing the geometric-constraint-based phase-unwrapping method [16] to unwrap the low-frequency phase pixel by pixel. The unwrapped low-frequency phase is further used to unwrap the high-frequency phase pixel by pixel for absolute 3D shape recovery. Our experimental data demonstrated the success of the proposed method. Since only two fringe patterns are used for absolute 3D shape measurement, this proposed method can be used to measure multiple moving objects at the same time.

Section 2 introduces the principles of modified FTP and our proposed framework of absolute phase retrieval. Section 3 illustrates the simulation result to verify the framework, and Section 4 presents some experimental validations to demonstrate the success of our proposed method. Finally, Section 5 summarizes this research.

2. PRINCIPLES

This section introduces the basic principles used in this research: (1) FTP, (2) modified FTP, (3) two-frequency absolute phase unwrapping, (4) the proposed method, and (5) robustness enhancement of phase unwrapping by using the geometric constraints of a DFP system.

A. FTP

The FTP method requires one single fringe pattern that can be described as

$$I(x,y) = I'(x,y) + I''(x,y)\cos[\phi(x,y)], \tag{1}$$

where $I'(x,y)$ represents the average intensity, $I''(x,y)$ the intensity modulation, and $\phi(x,y)$ the carrier phase. Equation (1) can be re-written as using Euler's formula:

$$I(x,y) = I'(x,y) + \frac{I''(x,y)}{2}[e^{j\phi(x,y)} + e^{-j\phi(x,y)}]. \tag{2}$$

The carrier signal can be obtained by applying a proper bandpass filtering:

$$I_f(x,y) = \frac{I''(x,y)}{2}e^{j\phi(x,y)}, \tag{3}$$

and the phase can be retrieved by

$$\phi(x,y) = \tan^{-1}\left\{\frac{\Im[I_f(x,y)]}{\Re[I_f(x,y)]}\right\}. \tag{4}$$

Here, $\Im[I_f(x,y)]$ and $\Re[I_f(x,y)]$, respectively, represent the imaginary and real parts of $I_f(x,y)$. Equation (4) provides phase values ranging from $-\pi$ to $+\pi$ with a modulus of 2π, and a spatial or temporal phase-unwrapping method is required to obtain continuous phase for 3D shape measurement.

B. Modified FTP

The FTP method works well if the surface geometry changes slowly and surface texture is not very rich. To improve the

performance of the FTP method, Guo *et al.* [6] proposed a modified FTP method that uses two π-shifted fringe patterns:

$$I_1 = I'(x,y) + I''(x,y)\cos[\phi(x,y)], \tag{5}$$

$$I_2 = I'(x,y) + I''(x,y)\cos[\phi(x,y)+\pi], \tag{6}$$

and taking the difference of two fringe patterns leads to

$$I_d = (I_1 - I_2) = 2I''(x,y)\cos[\phi(x,y)]. \tag{7}$$

A similar bandpass filtering can be used to retrieve the wrapped phase, similar to the single-pattern FTP method. By eliminating the impact of the DC component [i.e., $I'(x,y)$], the modified FTP method can obtain better quality phase.

C. Two-Frequency Absolute Phase-Unwrapping Method

The FTP or modified FTP method can retrieve wrapped phase, and typically a spatial or temporal phase unwrapping is necessary to generate a continuous phase map. Phase unwrapping essentially determines the number of 2π, $k(x,y)$, to be added per pixel:

$$\Phi(x,y) = \phi(x,y) + 2\pi \times k(x,y). \tag{8}$$

Typically, a spatial phase-unwrapping method gives only a relative number $k(x,y)$, and, thus, the unwrapped phase is relative phase; a temporal phase-unwrapping method provides a unique absolute number $k(x,y)$ for absolute phase retrieval.

To achieve high-speed 3D absolute shape measurement, it is desirable to use two frequencies to retrieve absolute phase. The two-frequency phase-unwrapping method works as follows. First, one can obtain two wrapped phase maps $\phi^l(x,y)$ and $\phi^h(x,y)$, from which one can generate the equivalent phase map:

$$\phi^{\text{eq}}(x,y) = \phi^l(x,y) - \phi^h(x,y) \bmod 2\pi. \tag{9}$$

Here, mod is the modulus operation. If ϕ^{eq} does not have any 2π discontinuities, it can be regarded as unwrapped phase, i.e.,

$$\Phi^{\text{eq}}(x,y) = \phi^{\text{eq}}(x,y). \tag{10}$$

The unwrapped phase can determine fringe order for high-frequency phase $\phi^h(x,y)$ pixel by pixel through

$$k(x,y) = \text{Round}\left[\frac{\Phi^{\text{eq}}(x,y)\frac{f^h}{f^{\text{eq}}} - \phi^h(x,y)}{2\pi}\right], \tag{11}$$

where Round() converts a floating point number to its closest integer number, f^h is the frequency of the high-frequency phase, and f^{eq} is the frequency of the equivalent phase map. Once fringe order is determined, the high-frequency phase map can be unwrapped pixel by pixel:

$$\Phi^h(x,y) = \phi^h(x,y) + k(x,y) \times 2\pi. \tag{12}$$

Here, $\Phi^h(x,y)$ denotes the finally unwrapped high-frequency phase.

D. Proposed Absolute Phase-Recovery Method

The proposed method uses two fringe patterns having different frequencies. We can reduce the DC component by shifting one of the fringe patterns by π. They are described as

$$I_1 = I'(x,y) + I''(x,y)\cos[2\pi f^l x], \tag{13}$$

$$I_2 = I'(x,y) + I''(x,y)\cos[2\pi f^h x + \pi], \tag{14}$$

assuming carrier signals vary along the x direction. Here, f^h and f^l, respectively, denote high and low frequency. Similarly, taking the difference of these two patterns yields

$$I_d = (I_1 - I_2) = I''(x,y)\{\cos[\phi^l(x,y)] + \cos[\phi^h(x,y)]\}. \tag{15}$$

Phase maps of both frequencies can be obtained by applying two separate bandpass filters on each component. Once these two phase maps are extracted, we can apply a two-frequency phase-unwrapping algorithm to unwrap the high-frequency phase pixel by pixel.

Figure 1 illustrates the differences between FTP, modified FTP, and our proposed method. Apparently, the fundamental difference between our proposed method and the conventional FTP method lies in the fact that our method requires two bandpass filters to respectively obtain the low- and high-frequency signals.

This absolute phase-recovery method works well in theory. However, Eq. (11) indicates that the two-frequency phase-unwrapping method could be very sensitive to noise if a large scaling factor f^h/f^{eq} is applied to the equivalent phase map. Such a problem deteriorates our proposed method since FTP requires the high-frequency signal to be as high as possible to recover details, yet the low frequency must be low enough such that one single period of fringe pattern covers the whole range of sensing. For a DFP system using a projector resolution of 1280×800, if the high-frequency signal uses a fringe period of 18 pixels, and the equivalent low-frequency signal uses a period of 800 pixels, the scaling factor is $f^h/f^{\text{eq}} \approx 44$, any phase noise larger than 0.07 rad could lead to incorrect fringe

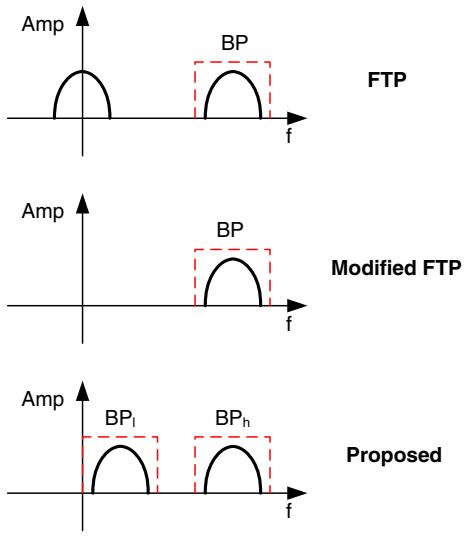

Fig. 1. Illustrations of different FTP methods. The top figure shows the standard FTP method that uses a bandpass filter to extract the carrier frequency signal that could be polluted with the DC signal; the middle figure shows no DC signals and a single bandpass filter for carrier frequency signal extraction; the bottom figure shows the proposed method that does not have a DC signal but requires two bandpass filters with one extracting the low-frequency carrier signal and the other extracting the high-frequency carrier signal.

order determination and, thus, wrong unwrapped phase. Subsection 2.E discusses our proposed computational framework to alleviate such a problem.

E. Robustness Enhancement by Using DFP System Geometric Constraints

To alleviate the impact of noise on fringe order determination, we propose to use more than one period of fringes to represent the equivalent low-frequency phase. The low-frequency phase is first temporally unwrapped by referring to virtually created minimum phase map using the geometric constraints of the DFP system. The pixel-by-pixel phase-unwrapping method has been thoroughly discussed by An *et al.* [17]; this subsection only briefly introduces the main idea that is applicable to this particular application.

Figure 2(a) illustrates the existence of a minimum phase map $\Phi_{\min}$ at a virtually defined depth $z = z_{\min}$ for a DFP system. Simple geometry shows that if the object is virtually placed at $z_{\min}$, there exists a one-to-one mapping between the camera captured area and the projection area, and the phase, named $\Phi_{\min}$ here, can be uniquely defined on the mapped projection area. If the real object is placed at z that is further away from the object, the mapped region on the projector changes accordingly, as illustrated in Fig. 2(b).

If z is not too far away from $z_{\min}$, the wrapped phase at z can be unwrapped pixel by pixel by referring to $\Phi_{\min}$. Figure 3 illustrates the conceptual idea of unwrapping two periodic fringe patterns using minimum phase. Figure 3(a) shows the wrapped phase of the object at z with 2π discontinuities. Figure 3(b) shows the continuous minimum phase map $\Phi_{\min}$ on the projector space. Figure 3(c) shows the cross sections of these phase maps. Assume the region inside of the dashed red bounding box is what the camera captures at $z = z_{\min}$, and the captured region is shifted to the area inside of the solid blue bounding boxes at z. Intuitively, both phase maps can be properly unwrapped by adding 2π if the phase is smaller than the corresponding point on phase map $\Phi_{\min}$.

Figure 4 shows cases that use minimum phase to unwrap phase from three or four periodic fringe patterns. One can observe that fringe order k can be determined by

$$2\pi \times (k-1) < \Phi_{\min} - \phi < 2\pi \times k, \tag{16}$$

or

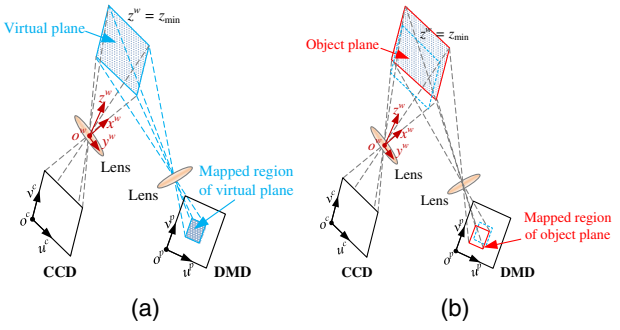

Fig. 2. Existence of minimum phase map of the DFP system [17]. (a) Mapped projection region for a virtual minimum plane $z = z_{\min}$; (b) mapped projection regions for an object at z.

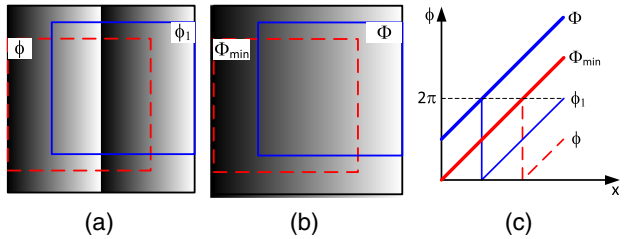

Fig. 3. Conceptual idea of unwrapping phase using the minimum phase map determined from geometric constraints [17]. (a) Windowed regions show the phase maps that are obtained by the camera at different depths: the red dashed window shows at $z_{\min}$ and the solid blue window shows at z; (b) corresponding $\Phi_{\min}$ and Φ on the projector; (c) cross sections of $\Phi_{\min}$ and Φ and the phase maps with 2π discontinuities.

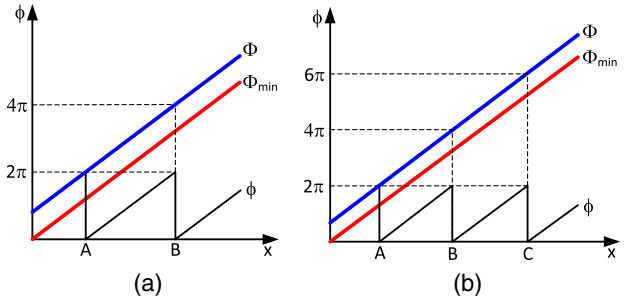

Fig. 4. Determination of number of 2π, or fringe order k, for periods of fringe patterns [17]. (a) Example of having three periods of fringe patterns, and (b) example of having four periods of fringe patterns.

$$k(x,y) = \text{ceil}\left[\frac{\Phi_{\min} - \phi}{2\pi}\right]. \tag{17}$$

Here, ceil[] is the ceiling operator that returns the closest upper integer value. By using this method, phase discontinuities are allowed for the low-frequency phase map, reducing noise impact. However, one should not increase the low frequency too much. Otherwise, it can pollute the high-frequency signal, decreasing phase quality and thus measurement quality.

3. SIMULATION

We performed simulations to demonstrate that the proposed method can reduce the effect of phase noise during the absolute phase recovery step. First, we simulated the case of the conventional two-frequency phase-unwrapping method where the single low-frequency fringe covers the entire sensing range. For this simulation, Gaussian noise with 20 signal-to-noise ratio (SNR) was added to all fringe patterns. Figure 5(a) shows the high-frequency sinusoidal fringe pattern with a period of $T^h = 20$, and Fig. 5(b) shows a close-up view of the fringe. We also generated a low-frequency fringe pattern with a period of $T^l = 768$, as shown in Fig. 5(c). Then, Fourier transform was performed to generate a frequency spectrum. Figure 6(a) shows both the frequency spectrum and bandpass filters we used. We selected two frequencies using the half Hanning

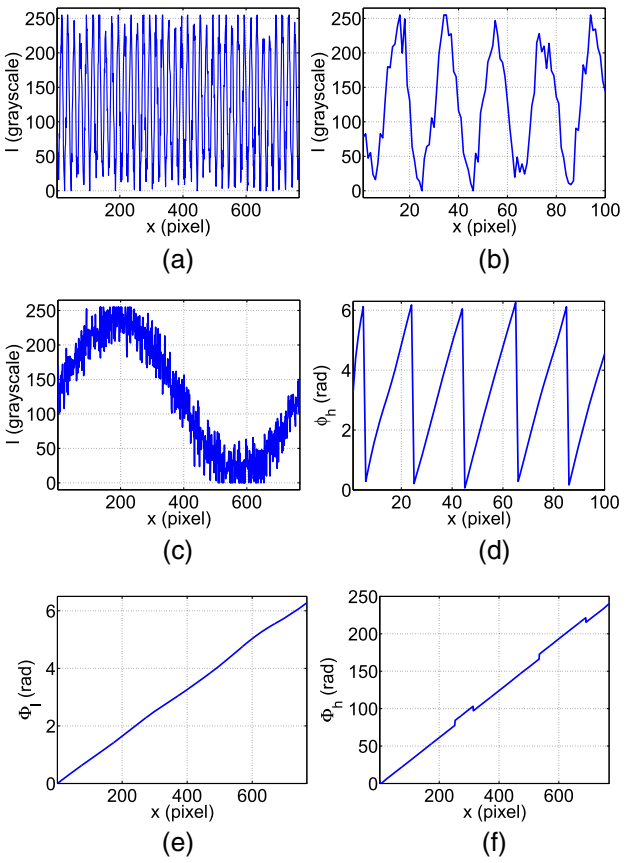

Fig. 5. Simulation results for the conventional two-frequency phase-unwrapping method where the single low-frequency fringe covers the entire sensing range (SNR = 20). (a) High-frequency fringe patterns with a fringe period of $T^h = 20$ pixels; (b) zoom-in view of fringe patterns shown in (a); (c) low-frequency fringe pattern with a fringe period of $T^l = 768$ pixels; (d) wrapped phase of the high-frequency fringe shown in (b); (e) wrapped phase of low-frequency fringe shown in (c); (f) unwrapped phase of the high-frequency fringe patterns using the low-frequency phase shown in (e).

windows as bandpass filters to retrieve phase maps for the high frequency [Fig. 5(d)] and the low frequency [Fig. 5(e)]. Because one period of low-frequency fringe pattern covers the whole sensing range, the low-frequency phase can be directly used to unwrap the high-frequency phase. Figure 5(f) shows the absolute phase after the unwrapping. Clearly, there are a few areas in which the phase is not properly unwrapped. This illustrates that if the ratio T^l/T^h is too high, the random noise could lead to incorrect fringe order k determination, failing to unwrap the high-frequency phase.

We then simulated the enhanced two-frequency phase-unwrapping method proposed in this paper with exactly the same setting (i.e., SNR = 20). In this simulation, we used a fringe period of $T^l = 768/3 = 256$ pixels for the low-frequency fringe, as shown in Fig. 7(a). We performed analysis similar to that used in the previous case. Figure 6(b) shows the frequency spectrum and bandpass filters we used to separate each frequency component. Since we used three periods for low-frequency fringe patterns, its frequency f^l has been increased, i.e., moved further away from the DC component.

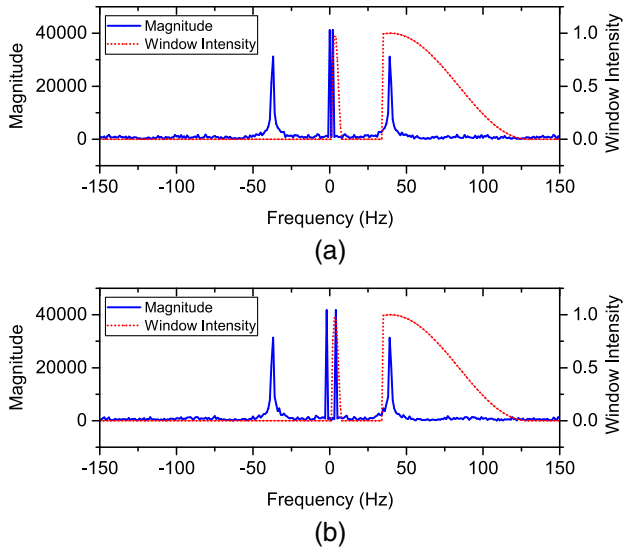

Fig. 6. Frequency spectrum and bandpass filters for FTP. (a) Two-frequency unwrapping method when the low-frequency fringe covers the whole sensing area ($T^l = 768$ pixels); (b) the proposed method ($T^l = 256$ pixels).

We generate the $\Phi_{\min}$ using the geometric-constraint approach presented by Hyun and Zhang [16], shown by the red dashed line in Fig. 7(b). The low-frequency phase is then unwrapped pixel by pixel using $\Phi_{\min}$. Figure 7(c) shows the unwrapped low-frequency phase. The high-frequency phase is then unwrapped pixel by pixel by applying the two-frequency temporal phase-unwrapping method. Figure 7(d) shows the result. This figure shows that the entire phase is properly unwrapped. This

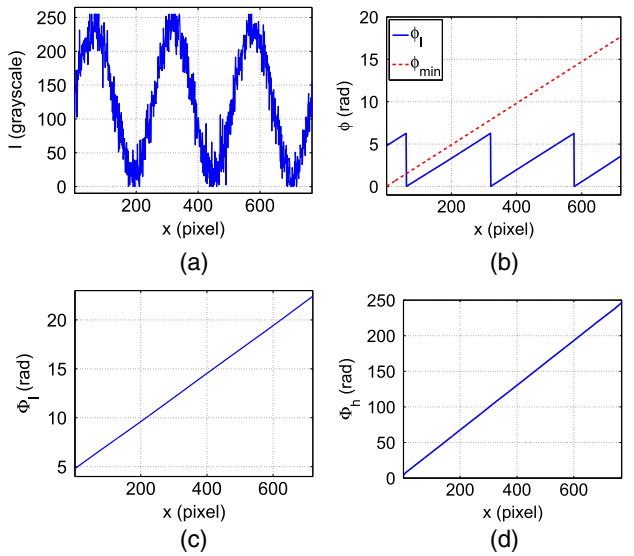

Fig. 7. Simulation results for the proposed method where we use more than one period of low-frequency fringe pattern (SNR = 20). (a) Low-frequency fringe patterns with a fringe period of $T^l = 256$ pixels; (b) wrapped phase of (a) and the minimum phase $\Phi_{\min}$; (c) unwrapped phase of low-frequency fringe patterns using $\Phi_{\min}$; (d) unwrapped phase of the high-frequency fringe patterns using the unwrapped low-frequency phase shown in (c).

is because, by using multiple periods of low-frequency fringe patterns, the ratio T^l/T^h is reduced to 1/3 of that of the previous method. These simulation results verified that our method indeed increases the robustness of the two-frequency phase-unwrapping algorithm, and can successfully perform pixel-by-pixel phase unwrapping for the modified FTP method under noisy conditions.

4. EXPERIMENT

We set up a structured light system to test our framework. It consists of a camera, which has a 1/1.2 in. complementary metal-oxide-semiconductor (CMOS) sensor (model: The Imaging Source DMK 23UX174), and a 2/3 in. imaging lens (model: Computar M1214-MP2) with a focal length of 12 mm and an aperture of F/1.4. We also used a digital light processing (DLP) projector (model: Dell M115HD) with a focal length of 14.95 mm and an aperture of F/2.0 to project fringe patterns to the object. Resolutions for the camera and the projector are 1024 × 768 pixels and 1280 × 800 pixels, respectively. We calibrated the system using the method developed by Li *et al.* [19].

We first tested our proposed method by measuring a Zeus statue, as shown in Fig. 8(a). We projected two fringes with different fringe pitches on the sculpture, and the face area is selected for further analysis. We used a fringe period of $T^h = 12$ pixels for the high-frequency fringe pattern. Figure 8(b) shows the captured fringe image. Two low-frequency fringe patterns are captured; Fig. 8(c) shows the fringe period of 800 pixels, and Fig. 8(d) shows the fringe period of $T^l = 84$ pixels. Since the projector's vertical resolution is $T^l = 800$ pixels, the single fringe for the former case ($T^l = 800$ pixels) covers the entire sensing range. Figures 8(e) and 8(f) show the difference image between these low-frequency fringe patterns and the high-frequency fringe pattern.

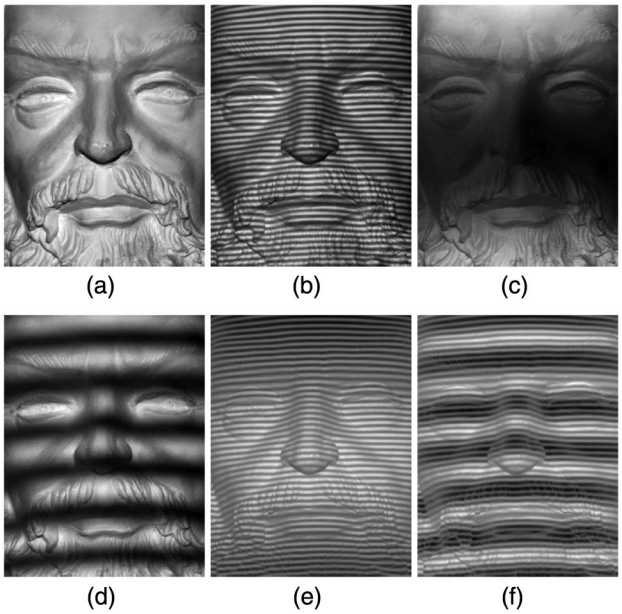

Fig. 8. Experimental results of measuring a Zeus statue with the proposed method and the conventional two-frequency temporal phase-unwrapping method. (a) Photograph of the object; (b) high-frequency fringe image ($T^h = 12$ pixels); (c) low-frequency fringe image ($T^l = 800$ pixels); (d) low-frequency fringe image ($T^l = 84$ pixels); (e) difference image I_d between (b) and (c); (f) difference image between (b) and (d).

Figure 9 shows the frequency spectrum of difference fringe maps after applying the Fourier transform. The position of the high-frequency component is the same for both cases since we used the same fringe period ($T^h = 12$ pixels) for the high-frequency fringe pattern. When the low-frequency fringe period is $T^l = 800$ pixels, as shown in Fig. 9(a), the low-frequency peak is only one pixel away from the DC component (i.e., center of the image). Since one period of the fringe pattern is used, it is almost impossible for this case to satisfy the fundamental assumption of Fourier transform, i.e., the signal repeating itself to infinity. Therefore, the DC component is very obvious after taking the difference, making it difficult to separate the low-frequency component from the DC component using the bandpass filter. As a comparison, when the low-frequency fringe period is $T^l = 84$ pixels, as shown in Fig. 9(b), the low frequency moves further away from the DC component. Because more than one fringe period is used, this case also better satisfies the Fourier periodic assumption, leading to a substantially reduced DC signal.

Following the same procedures as discussed in Section 3, we can extract the wrapped phase for low-frequency phase and high-frequency phase by using two bandpass filters. Figure 10 shows the results. Figures 10(a) and 10(b) show phase maps that were extracted from both high- and low-frequency components when we used fringe periods of $T^h = 12$ pixels and $T^l = 800$ pixels. Since the low-frequency fringe period is long enough to cover the whole sensing range, its phase map is already continuous. Conceptually, we can directly use this map to unwrap the high-frequency phase pixel by pixel. Figure 10(c) shows the unwrapped phase map.

Different from the previous case, when two fringe periods ($T^h = 12$ pixels and $T^l = 84$ pixels) are used, the high-frequency phase map, shown in Fig. 10(d), is the same, but the low-frequency phase map, shown in Fig. 10(e), is no longer continuous. As discussed in Subsection 2.E, we used the geometric constraints of the structured light system to unwrap the low-frequency phase first. To do so, we generated a minimum phase map $\Phi_{\min}$ at $z = 540$ mm, which is the minimum distance between the object and the origin of the world coordinate (i.e., the camera lens center). Once the low-frequency phase is unwrapped with $\Phi_{\min}$, the high-frequency phase can then be

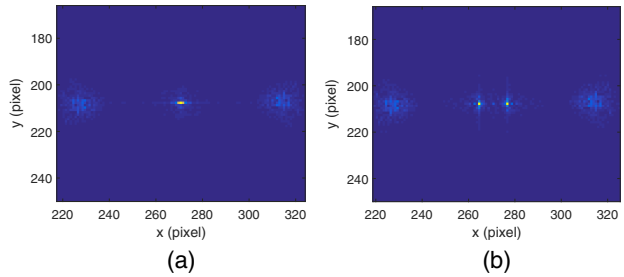

Fig. 9. Frequency spectrum maps of the difference fringe image. (a) Conventional two-frequency temporal phase-unwrapping method ($T^h = 12$ pixels, $T^l = 800$ pixels); (b) the proposed method ($T^h = 12$ pixels, $T^l = 84$ pixels).

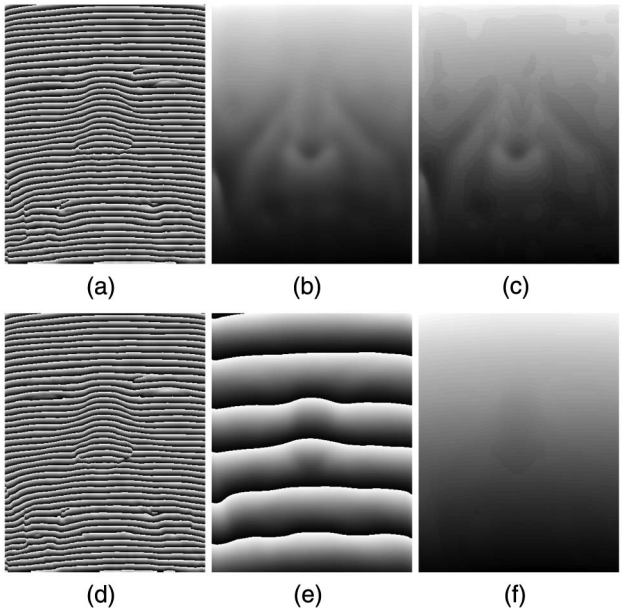

Fig. 10. Extracted low- and high-frequency phase from the frequency spectrum map shown in Fig. 9. (a) High-frequency wrapped phase map for $T^h = 12$ pixels and $T^l = 800$ pixels; (b) low-frequency wrapped phase map for $T^h = 12$ pixels and $T^l = 800$ pixels; (c) unwrapped phase using the phase map shown in (a) to unwrap the phase map shown in (b); (d) high-frequency wrapped phase map for $T^h = 12$ pixels and $T^l = 84$ pixels; (e) low-frequency wrapped phase map for $T^h = 12$ pixels and $T^l = 84$ pixels; (f) unwrapped phase using the phase map shown in (e) to unwrap the phase map shown in (d).

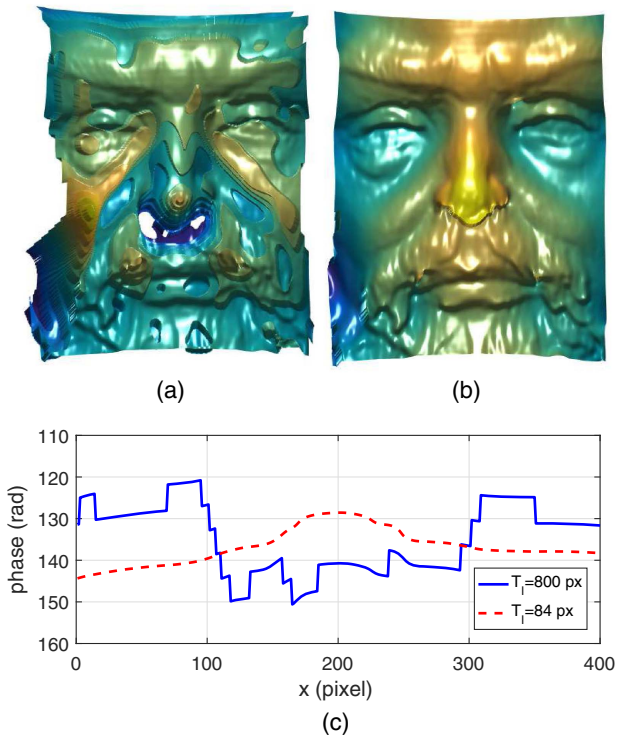

Fig. 11. 3D reconstruction results of the Zeus sculpture with different low-frequency fringe periods. (a) 3D reconstruction result using the phase map shown in Fig. 10(c); (b) 3D reconstruction result using the phase map shown in Fig. 10(f); (c) horizontal cross sections of absolute phase maps near the nose ridge of the object.

unwrapped pixel by pixel. Figure 10(f) shows the unwrapped phase. Compared with the unwrapped phase shown in Fig. 10(c) from the low-frequency period $T^l = 800$ pixels, this unwrapped phase is much smoother.

Once the unwrapped phase is obtained, the 3D shape can be recovered. Figure 11 shows the reconstructed 3D geometries. One may observe that when we use the low-frequency fringe period $T^l = 800$ pixels, the absolute phase map shows apparent discontinuities, and the reconstructed 3D geometry is not correct. This is because the fringe period ratio T^l/T^h in this case is $800/12 = 66.6$, which is very large, failing the fringe order detection. In contrast, when we reduce the low-frequency fringe period to $T^l = 84$ pixels, the ratio $T^l/T^h = 84/12 = 7$ is substantially smaller; and thus we can successfully unwrap the phase and then reconstruct the 3D geometry. To better illustrate the difference, Fig. 11(c) shows horizontal cross sections of the absolute phase maps near the nose ridge region of the object. These experiments demonstrated that the enhanced phase-unwrapping approach indeed can increase the robustness of the absolute phase unwrapping for the FTP method.

Since only two fringe patterns are required to recover the 3D absolute shape, the proposed method can be used to measure rapidly moving objects. We set up a new high-speed 3D shape measurement system that consists of a high-speed CMOS camera (model: Phantom V9.1) with 1024×786 resolution, and a DLP projector (model: LightCrafter 4500) with 912×1140 resolution. The camera's lens has a focal length of 24 mm and aperture of F/1.8. To achieve fast projection speed, we used 1 bit binary patterns instead of gray-scale ones. For the high-frequency fringe pattern ($T^h = 12$ pixels), we used the binary area modulation pattern developed by Lohry and Zhang [20] to reduce the impact of the third-order harmonics; and for the low-frequency fringe pattern ($T^l = 84$ pixels), we used the binary dithered pattern.

We measured falling ping pong balls to prove the ability of our method to measure multiple rapidly moving objects. We projected two periods of fringe patterns with $T^h = 12$ pixels and $T^l = 84$ pixels at 1.5 kHz, and the precisely synchronized camera to capture images at the same frame rate. Figures 12(a) and 12(b) show the example high- and low-frequency fringe images. We segmented each ping pong ball and applied the proposed method to unwrap each ping pong ball independently. Figure 12(c) and Visualization 1 show the measurement results. This experiment demonstrated that our proposed method can be used to measure multiple rapidly moving objects.

We further experimentally evaluated the capability of our proposed method comparing with the single-shot method developed by Li *et al.* [18]. In this experiment, we simultaneously measured a sculpture and a large sphere, as shown in Fig. 13(a). Again, we projected high- and low-frequency fringes with the same periods ($T^h = 12$ pixels and $T^l = 84$ pixels) as those used for the ping pong ball measurements. For the single-shot FTP, only the high-frequency fringe image was used

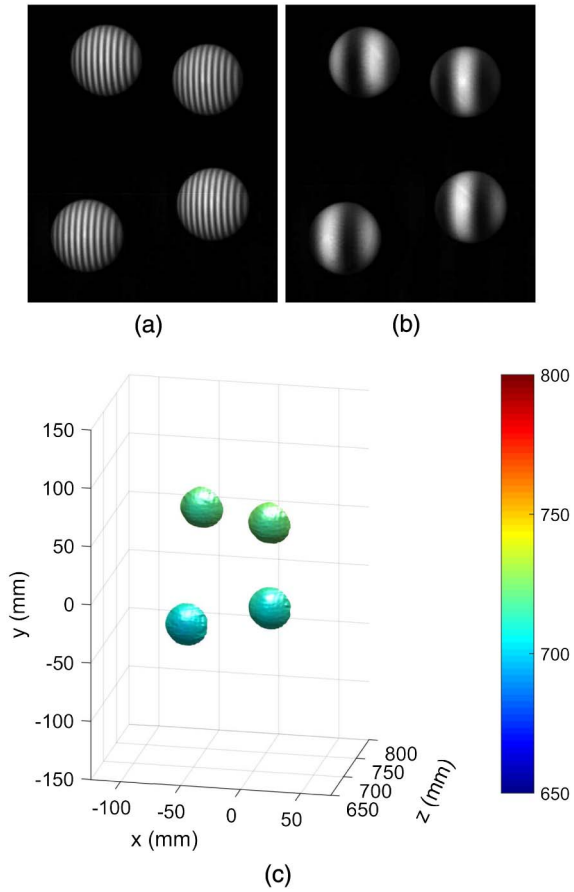

Fig. 12. High-speed 3D shape measurement of falling ping pong balls with the proposed method (see Visualization 1). (a) One representative high-frequency fringe image ($T^h = 12$ pixels); (b) one representative low-frequency fringe image ($T^l = 84$ pixels); (c) reconstructed 3D geometry.

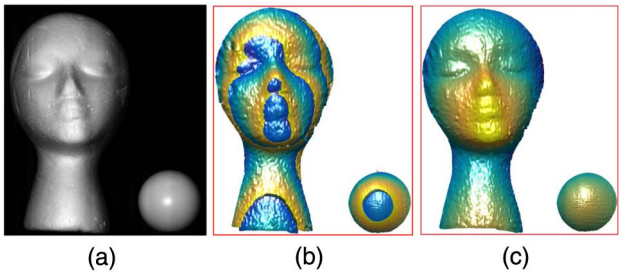

Fig. 13. 3D measurement using the proposed method and the single-shot method proposed by Li *et al.* [18]. (a) Photograph of the objects; (b) 3D measurement result using the single-shot FTP method proposed by Li *et al.* [18]; (c) 3D measurement result using our proposed method.

for 3D reconstruction. We used the modified FTP method on a sculpture and a ball separately to minimize the phase distortion due to background. Figure 13(b) shows the result using the single-shot method developed by Li *et al.* [18]; and Fig. 13(c) shows the result using our proposed method. One can clearly see that the result obtained from Li's method has discontinuous areas on both objects, indicating that the measurement depth range goes beyond the depth limitation of the geometric-constraint-based phase-unwrapping method [17]. In contrast, our proposed method has substantially larger depth range (approximately 7 times) than the single-shot method due to the use of the low-frequency fringe pattern, albeit the measurement speed is reduced.

5. SUMMARY

In summary, this paper has presented a new method for pixel-by-pixel absolute phase recovery with the modified Fourier transform method. This method uses one low-frequency fringe pattern and one high-frequency fringe pattern, and the phase obtained from the low-frequency fringe pattern is used to temporarily unwrap the phase obtained from the high-frequency fringe pattern. Because of the fundamental limitation of Fourier transform and the impact of noise on the temporal phase-unwrapping method, our simulation and experimental results demonstrated that it is difficult to use the low-frequency fringe pattern with a single fringe period covering the entire sensing range. To overcome this problem, we implemented the novel geometric-constraint-based phase-unwrapping method to unwrap the low-frequency phase. By this means, the low-frequency fringe pattern can decrease its fringe period such that higher quality phase can be obtained. Also, the noise impact on the temporal phase unwrapping can be alleviated. Since the proposed method can unwrap phase temporally, we demonstrated that our proposed method can be used to simultaneously measure multiple objects; and because our proposed method uses only two fringe patterns for 3D shape reconstruction, we also demonstrated that our proposed method can be employed for high-speed applications. Comparing with the single-shot FFT method developed by Li *et al.* [18], the proposed method can effectively increase its depth measurement range by a factor of approximately 7.

Acknowledgment. We would like to thank other students in our lab for their kind advice in the research.

REFERENCES

1. M. Takeda and K. Mutoh, "Fourier transform profilometry for the automatic measurement of 3-D object shapes," Appl. Opt. **22**, 3977–3982 (1983).
2. X. Su and Q. Zhang, "Dynamic 3-D shape measurement method: a review," Opt. Laser. Eng. **48**, 191–204 (2010).
3. M. Takeda, "Fourier fringe analysis and its applications to metrology of extreme physical phenomena: a review," Appl. Opt. **52**, 20–29 (2013).
4. M. B. Whitworth and J. M. Huntley, "Dynamic stress analysis by high-resolution reflection moiré photography," Opt. Eng. **33**, 924–931 (1994).
5. S. Petitgrand, R. Yahiaoui, K. Danaie, A. Bosseboeuf, and J. Gilles, "3D measurement of micromechanical devices vibration mode shapes with a stroboscopic interferometric microscope," Opt. Lasers Eng. **36**, 77–101 (2001).
6. L. Guo, X. Su, and J. Li, "Improved Fourier transform profilometry for the automatic measurement of 3D object shapes," Opt. Eng. **29**, 1439–1444 (1990).
7. H. Guo and P. S. Huang, "Absolute phase technique for the Fourier transform method," Opt. Eng. **48**, 043609 (2009).

8. B. Budianto, P. Lun, and T.-C. Hsung, "Marker encoded fringe projection profilometry for efficient 3D model acquisition," Appl. Opt. **53**, 7442–7453 (2014).
9. Y.-Y. Cheng and J. C. Wyant, "Two-wavelength phase shifting interferometry," Appl. Opt. **23**, 4539–4543 (1984).
10. H. Zhao, W. Chen, and Y. Tan, "Phase-unwrapping algorithm for the measurement of three-dimensional object shapes," Appl. Opt. **33**, 4497–4500 (1994).
11. K. Creath, "Step height measurement using two-wavelength phase-shifting interferometry," Appl. Opt. **26**, 2810–2816 (1987).
12. Y.-Y. Cheng and J. C. Wyant, "Multiple-wavelength phase shifting interferometry," Appl. Opt. **24**, 804–807 (1985).
13. D. P. Towers, J. D. C. Jones, and C. E. Towers, "Optimum frequency selection in multi-frequency interferometry," Opt. Lett. **28**, 887–889 (2003).
14. G. Sansoni, M. Carocci, and R. Rodella, "Three-dimensional vision based on a combination of gray-code and phase-shift light projection: analysis and compensation of the systematic errors," Appl. Opt. **38**, 6565–6573 (1999).
15. S. Zhang, *High-Speed 3D Imaging with Digital Fringe Projection Technique*, 1st ed. (CRC Press, 2016).
16. J.-S. Hyun and S. Zhang, "Enhanced two-frequency phase-shifting method," Appl. Opt. **55**, 4395–4401 (2016).
17. Y. An, J.-S. Hyun, and S. Zhang, "Pixel-wise absolute phase unwrapping using geometric constraints of structured light system," Opt. Express **24**, 18445–18459 (2016).
18. B. Li, Y. An, and S. Zhang, "Single-shot absolute 3D shape measurement with Fourier transform profilometry," Appl. Opt. **55**, 5219–5225 (2016).
19. B. Li, N. Karpinsky, and S. Zhang, "Novel calibration method for structured light system with an out-of-focus projector," Appl. Opt. **53**, 3415–3426 (2014).
20. W. Lohry and S. Zhang, "Fourier transform profilometry using a binary area modulation technique," Opt. Eng. **51**, 113602 (2012).